JOURNAL OF MATERIALS SCIENCE **35** (2000) 5465–5474

Investigating the influence of fabrication process and crystal orientation on shear strength of silicon microcomponents

QUANFANG CHEN, DA-JENG YAO, CHANG-JIN KIM, G. P. CARMAN
Mechanical and Aerospace Engineering Departments, University of California, Los Angeles, USA
E-mail: carman@seas.ucla.edu

A summary of the influence of microfabrication processes (wet and dry etching) and crystal orientation on the effective shear strength of microridges is addressed in this paper. Test results indicate that both crystal orientation and geometry plays an important role in determining the strength. The largest shear strengths obtained were for triangular and rectangular ridges fabricated with wet etching and deep RIE respectively. Both of these structures had similar crystal orientations. These strength values were approximately 3.5 times larger than the lowest strengths measured for wet etching structures. Using Chlorine RIE, we were able to demonstrate the influence of crystal orientation on strength, with microridges of {110} sidewall made on a (100) wafer the largest. For wet etching, we found that the strength was concentration dependent. For example, a 45% KOH fabricated structure produced strength values 65% higher than 30% KOH fabricated ones (note crystal orientation the same). This was attributed to a geometric effect, that is the 45% KOH solution had a "V" shaped bottom while the 30% KOH had a flat bottom. EDP and TMAH values had similar strengths to the 30% KOH solution (note similar crystal orientation). Therefore, microcomponent strength is strongly dependent upon fabrication process as well as crystal orientation. © *2000 Kluwer Academic Publishers*

1. Introduction

Strength and durability are two important issues for engineers using micro-electro-mechanical-systems (MEMS) components, in particular those supporting mechanical loads. One example is a mesoscale inchworm motor using microfabricated microridges to transfer mechanical loads in excess of 500 N [1]. Load bearing applications such as this raise the question as to the strength and fatigue life associated with microfabricated components.

Silicon is the predominant material currently being used in the MEMS field. This is due to the well-understood microfabrication processes that are borrowed from integrated circuits (IC) manufacturing. Fabrication of micro components often involves carving out three-dimensional shapes from the silicon wafer by a series of lithography and etching steps. In general, anisotropic etching (i.e., directional etching) techniques are widely used to obtain the three-dimensional geometry from single crystal silicon. Since etching is the result of a chemical reaction between the material (silicon) and the etchant, the surface geometry varies significantly among different etchants and processing conditions. While some data are available on strength properties of micro components made from specific processes, they are incomplete for understanding the influence of different micromachining process on strength. For example, a component made by an anisotropic wet etching method may provide strengths distinctly different from a component fabricated by an isotropic wet etching or an anisotropic dry etching method (as discussed in this paper).

Another phenomenon associated with the chemical-etching process is the dependence of etching rate on crystal orientations (anisotropic). The crystal orientation dependent etching rates vary greatly among crystal directions (e.g. 150 time's difference in etching between ⟨111⟩ and ⟨110⟩ for KOH solution [2]). The etching rate and the crystal orientation on the wafer determine the final three-dimensional profile. Therefore, different alignments (crystal orientation) during fabrication (etching rate dependent) may produce different strengths of a component structure.

Notable studies of microscale strength testing include those (not limited to) by bending a micro cantilever with a stylus [3, 4], by resonating thin beam structures [5, 6], by using micromachined built-in levers [7], and by tensile test [8]. While these test data provide useful information, the vast majority was intended to provide the intrinsic properties of the material rather than strength properties that are due to either processing or architecture. Therefore, very little data is available detailing the influence of manufacturing processes and crystal

© *2000 Kluwer Academic Publishers*

orientation on strength of the microfabricated components.

The objective of this study is to investigate the influence of different microfabrication methods (wet and dry etching, e.g., KOH, EDP, TMAH, reactive ion etching (chlorine RIE and deep RIE) and crystal orientations ({111}, {110}, and {100} sidewall surfaces) on the effective shear strength of single crystal silicon microridges. The microridge's geometry was chosen based on both the of micromachining techniques used to fabricate the geometry and the proposed use in a mesoscale inchworm motor [1].

2. Specimen preparation

The architecture shape of microridge (made of single crystal silicon) is rectangular in cross section with the size of 4.5 μm in wide, 5 μm in height, 3 mm long, and a pitch of 10 μm (Fig. 1a and b). This specific size was dictated both by limitations of our lithography facility and requirements for a mesoscale inchworm motor [1]. While smaller sizes are possible, they would cause additional complications that may not add further insight into the proposed investigation. A pair of 3 mm by 5 mm silicon chips is engaged (Fig. 1c) to measure the shear strength (load bearing capability) between the two chips. A trapezoid shape microridge was also fabricated and tested in a similar fashion (Fig. d) and the size of ridge is 2 μm on top and 9 μm at bottom with a pitch of 11 μm. The test setup is described later in this paper.

2.1. Fabrication by wet anisotropic etching

Three different wet anisotropic etchants were used to study different etching conditions. These are KOH (30% and 45% at 70 °C), EDP (Ethylenediamine and Pyrocatechol, PSE-300 of Transene Co. at 100 °C), and TMAH (Tetramethylammonium Hydroxide, 25% in water, Moses Lake Industries, at 85 °C). During each of these fabrications processes the microridge pattern is oriented parallel to the intersection between the wafer top surface ({110} plane) and vertical plane ({111}) that form the microridges' sidewall of {111} plane; in other words, the microridges will be formed by {110} top surface and {111} vertical surfaces (sidewall).

The general processing steps for wet etching are as follows.

(1) Deposit 1500 Å thick silicon nitride (Si_3N_4) on (110) or (100) type silicon wafer by LPCVD.
(2) Spin coat photoresist and define the microridge pattern with lithography.
(3) Etch and pattern Si_3N_4 with RIE ($CF_4 + O_2$, 5 : 1), Strip off photoresist.
(4) Wet anisotropic etching (30% KOH or 45% KOH at 70 °C, 25% TMAH at 85 °C, or EDP at 100 °C)
(5) Dice wafer to 3 mm × 5 mm chips

The wet-etching processes described above with a (110) silicon wafer produce essentially the same transverse section shape (rectangular) microridges with the same crystallographic orientation (ridges along with {110}/{111} intersection). However, there is a discrepancy in the trench surface that requires comment. Three of the four wet etchants (30% KOH, TMAH and EDP solution) produce rectangular ridges with vertical sidewalls mounted on a flat bottom base as shown in Fig. 2. However, the 45% KOH solution produces rectangular ridges with vertical sidewalls mounted on a sloped ("V" shaped) bottom surface that resembles a triangular cross section as shown in Fig. 3 and reported in [9]. An additional concern is the variation in microridge size for different etching processes. It is known that the lateral etching rate of KOH and EDP are roughly comparable under certain condition [2]. For EDP, the {110}/{111} etching rate ratio is 30 : 1–150 : 1; while for KOH it is 50 : 1–160 : 1, with exact values depending on the composition and temperature [2, 9]. For TMAH, the {110}/{111} etching rate ratio is 36 : 1–59 : 1 [10, 11]. Based on these numbers, the variations in microridge width due to lateral etching are between ∼0.1 μm (KOH) to ∼0.3 μm (TMAH and EDP) for

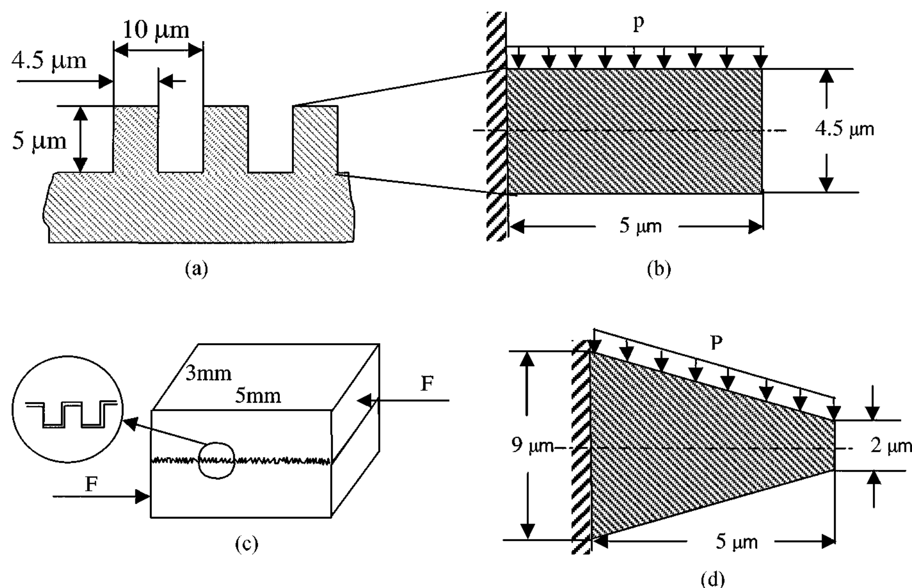

Figure 1 Test specimen. (a) Rectangular ridges; (b) Microridges under load; (c) Engagement under load; (d) Trapezoid ridges.

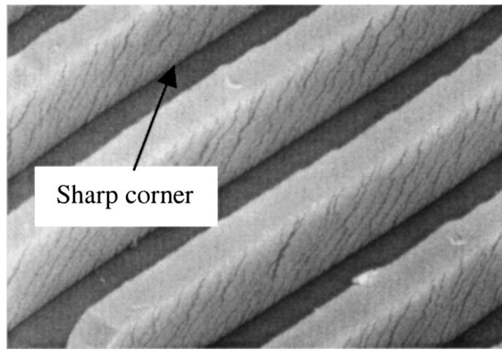

Figure 2 Microridges made on (110) wafer by 30% KOH at 70 °C.

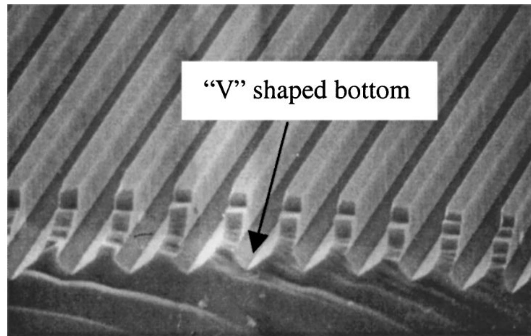

Figure 3 Microridges made on (110) wafer by 45% KOH at 70 °C.

etching depths of 5 μm. Using Kirchoff beam assumptions and modeling the influence of width on stress distribution, the variations in physical size cause stress changes are less than 9%. During the fabrication process of samples, the microridge height variations were controlled to be less than 0.2 μm. Using a similar approach, the stress changes are predicting to be less than 8%. Therefore, one expects negligible disparities (less than 10%) in strength caused by the variations in the cross sectional dimensions of the ridges.

In addition to rectangular shapes, wet etching can also produce trapezoid shape microridges. Fundamentally, all the wet etching methods described above could produce trapezoid shape ridges but we focused on a 30% KOH solution in this document. The fabrication process is the same except that the crystal orientation is different. In the trapezoid case, ridges are aligned with the intersection of {110} and {100} on a (100) silicon wafer instead of aligning with {111}/{110} intersection on a (110) wafer. The microridge is formed by {100} plane (top surface) and {111} sidewall. The size of this microridge structure are 5 μm in height, 2 μm on top and 9 μm on bottom with a pitch of 11 μm (Figs 1d and 4). The lateral etching is smaller than previously mentioned. While the shape is fundamentally different with a different crystal orientation, the results provide an indication of strength variation that might be expected from different structures.

2.2. Fabrication by chlorine RIE

Chlorine RIE was also used to fabricate rectangular microridges in this research. One advantage of using RIE over anisotropic wet etching is that there is no obvious difference in etching rate between crystal planes facing the ion beam. In other words, microridges can be made in any predefined crystal orientation on the wafer with little variation in shape. This provides an opportunity to determine the influence of crystal orientation on structural strength properties. In this study, we used two different wafers ((100) and (110)) to produce microridges along with three different crystallographic orientations: intersections of {100}/{100}, {100}/{110}, and {110}/{111}. Therefore, the {110}/{111} alignment was identical to the wet etching approach. The fabrication process is as follows.

(1) Spin coat photoresist and define microridge pattern with lithography.
(2) Evaporate 1000 Å nickel in thickness on silicon wafer.
(3) Remove photoresist and complete microridge patterning by lift-off process.
(4) Chlorine RIE etching of silicon using nickel pattern as etching mask.
(5) Dice wafer to 3 mm × 5 mm chips.

Every batch of wafers (including those patterned aligned with {100}/{100}, {100]/{110}, and {110}/{111} orientation) were etched at the same time in one chamber, therefore processing conditions were identical for the wafers. When reviewing the microridge geometry produced with each orientation, there was no obvious size difference between samples and the size was comparable with the wet etching approaches.

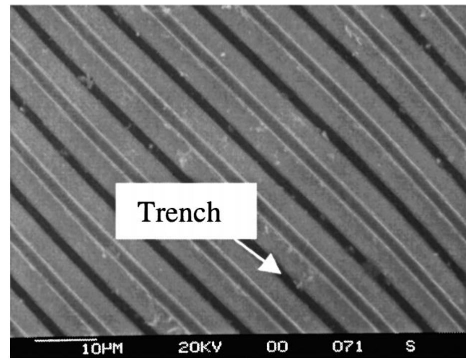

Figure 4 Trapezoid shape microridges made 30% KOH on (100) wafer (top view).

2.3. Fabrication by deep RIE

A deep RIE process based on inductive coil plasma (ICP) technology (PlasmaTherm) was also used in this study to investigate strength issue. The microridges were aligned with the intersection of {100}/{110}, an aligning that was similar to one of the chlorine RIE case but different from the wet etching structure. The fabrication process is as follows.

(1) Spin coat photoresist and define microridge pattern with lithography.
(2) Deep RIE etching.
(3) Strip off photoresist.
(4) Dice wafer to 3 mm × 5 mm chips.

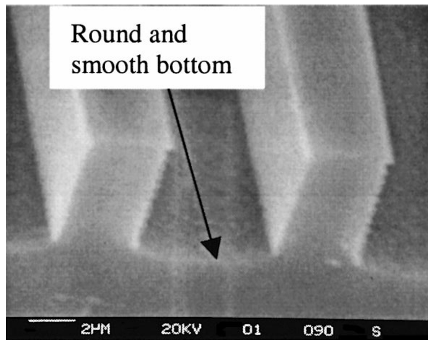

Figure 5 Microridges made by deep RIE.

The rectangular shape ridges were fabricated by deep RIE and the morphology is shown in Fig. 5. A rounded shape and smooth surface at bottom obtained with this deep RIE process is visible. The size of deep RIE fabricated microridges is very uniform with little due to the negligible lateral etching during fabrication. The size was comparable with chlorine RIE mentioned in preceding section and wet etching structure.

3. Test results and diccussion

3.1. Loading test setup

The test setup is schematically depicted in Fig. 6. A pair of 3 mm by 5 mm sample chips containing interlocking microridges is engaged. The maximum gap between engaged ridges is 1 μm, while the length of each ridge is 3 mm. When engaged, approximately four hundred sets of 3 mm long microridges transmit the load from one set of ridges to the other. While it may appear that engaging these ridges is time consuming due to alignment problems, previous research has demonstrated that this can be done in a relatively short period without impacting the ridge structure [1]. Precision issues related to lithographic techniques suggests that contact between engaged ridges is fairly uniform from ridge to ridge and along the length so that each ridge supports a comparable load when engaged.

An electromechanical load frame (Instron 5544) is used to apply mechanical load to the specimen and a data acquisition system records both load and displacement. In these tests a vertical force is applied to the specimen until failure occurs (loading rate is 25 μm/min).

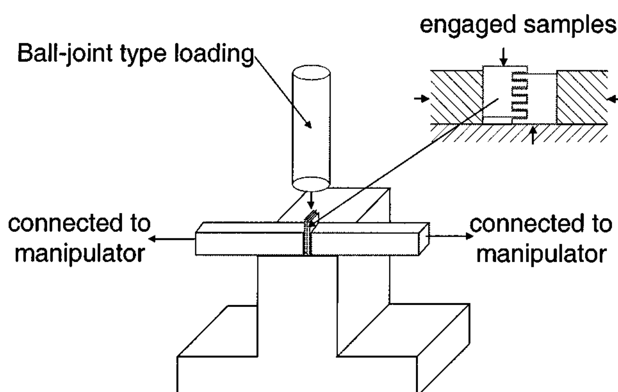

Figure 6 Setup for micro interlocking strength test.

A ball joint built into the cross head is used to minimize lateral loading forces on the specimen. A minimum of five samples per group is tested. The ultimate load divided by the engaged cross sectional area (3 mm × 5 mm) defines the effective shear strength values published in this document. For each specimen tested the engaged cross-sectional area is identical. While other approaches exist to define strength values for such component, we believe that the adopted definition is an appropriate one for structural application.

3.2. Results and discussion

A summary of strength data is presented in Table I and Fig. 7. We begin the discussion by evaluating the results obtained on the wet etching techniques using KOH solutions. Second we will compare the strengths obtained with EDP and TMAH solutions. Third we will discuss the strength difference between microridges with {111} sidewall on (110) wafer, and both {110} and {100} sidewalls on (100) wafer fabricated with chlorine RIE. Next we will discuss the strength obtained from deep RIE method with {110} sidewall on (100) wafer (note different crystal orientation than wet etching). Finally we will discuss the strength of trapezoid shape ridges with tilted {111} sidewall on (100) wafer. The trapezoid shape is discussed last due to the distinct difference in geometry when comparing with the other fabrication processes.

3.2.1. Strength of microridges made with KOH solutions

In general the strength of the microridges obtained by using KOH as etchant on (110) wafer is dependent on the concentration of KOH solution (see Table I and Fig. 7). The 45% KOH produces a substantially higher strength value (16.1 MPa), or 65% higher when compared with 30% KOH (9.6 MPa). We attribute the strength difference to the stress concentration that arises near the corner between the sidewall and base [9]. The 30% KOH solution produces a sharp bottom corner

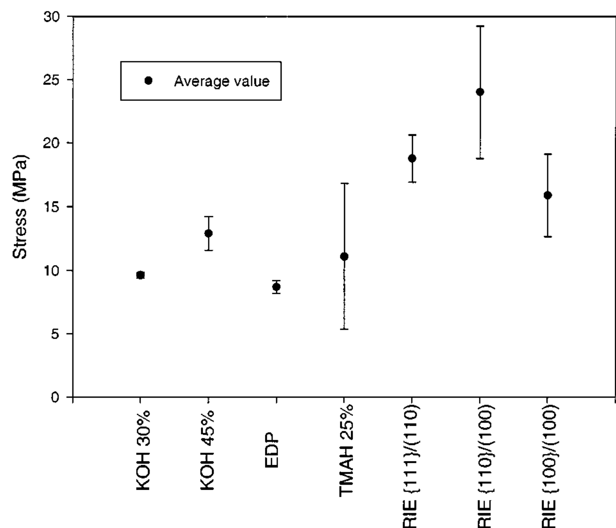

Figure 7 Strength values made by different fabrication process and crystal orientations.

TABLE I Average strength values for different fabrication processes and crystal orientations (MPa)

30% KOH {111}/(110)	45% KOH {111}/(110)	EDP {111}/(110)	TMAH {111}/(110)	RIE {111}/(110)	RIE {110}/(100)	RIE {100}/(100)	DRIE {110}/(110)	Trapezoid {111}/(100)
9.62 MPa	16.13 MPa	9.46 Mpa	11.08 MPa	18.78 MPa	26.39 MPa	14.63 MPa	34.1 MPa	37.4 MPa

Note: {111}/(110) means that microridges are made on a (110) wafer with sidewall of {111}. Loading is perpendicular to the sidewall, i.e., in ⟨111⟩ direction.

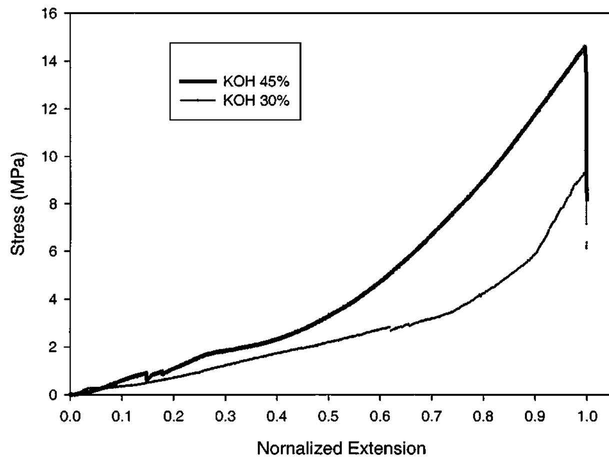

Figure 8 Measured stress curve versues normalized extension for 30% KOH and 45% KOH etching.

(Fig. 2), while the 45% KOH produces a corner with a wider angle ("V" shaped, Fig. 3). The wider angle (by 45% KOH solution) dramatically reduces the stress concentration [12] and thereby increases the strength of the microridge structure.

In Fig. 8, strength test results versus normalized displacement for two representative samples etched with 30% KOH and 45% KOH are presented. The displacement values are normalized to the displacement recorded at failure for each etching process. The total displacements recorded during the test represents a combination of machine, fixture, and specimen displacements, therefore stiffness cannot be inferred from this plot. The fairly smooth loading profile indicates that the ridges do not fail until ultimate strength is reached. Initials minus load drops are simply related to seating the specimen. If the ridges were breaking during the loading sequence, the curve should display distributed load drops but this was not observed in any of the samples. For the 30% KOH etched sample (Fig. 8), the strength rises to a maximum of 9.5 MPa at which time failure of the ridges occurs. Prior to this load level, no apparent damage was found. For the 45% KOH etched sample, the strength rises to 15 MPa.

SEM micrographs of failure surfaces are presented in Fig. 9 for 30% KOH etched samples and Fig. 10 for 45% KOH. Fig. 9a is a pair of mating chips tested. Results indicate that all engaging microridges on the bottom piece were broken off and remain within the top piece. The magnification of broken ridges on the bottom piece shows that the {111} crystallographic planes define the failure surface (Fig. 9b). The adjacent {111} planes cover the failure surface and form repeating triangular shapes, as shown in Fig. 9b, where the bottom piece of Fig. 9a has been rotated to reveal the presence of these triangular shapes. The angle between the actual loading vector (Fig. 1b) and the inclined {111} (forming triangular shape in Fig. 9b) is 19.5° indicating that 95 of the load applied is distributed in shear along the {111} plane. The {111} crystallographic plane is reported to

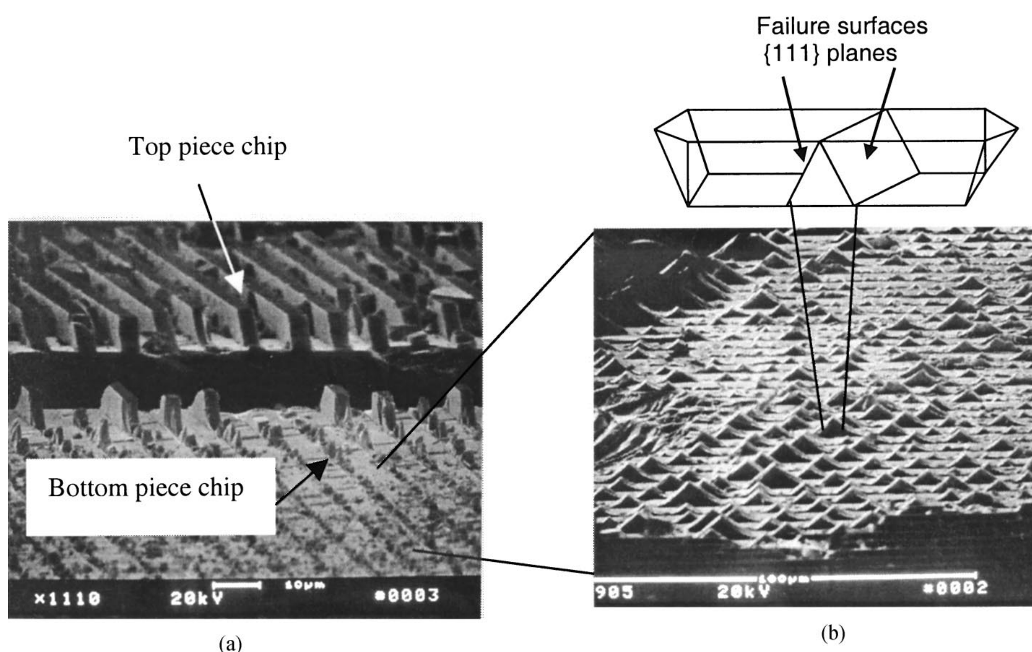

Figure 9 (a) Morphology of broken microridges prepared by 30% KOH after fracture, two pieces. (b) Enlarged views of bottom piece. Triangular shapes are formed by {111} planes.

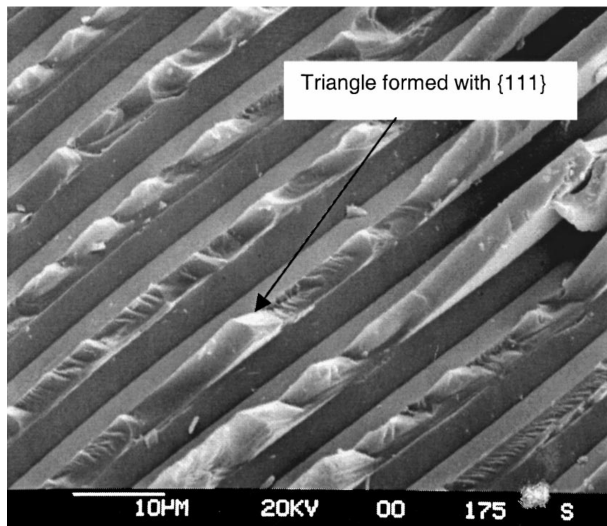

Figure 10 Morphology of broken microridges with 45% KOH after fracture, bank shape basement.

be the sliding plane with a low shear strength value [13] suggested a low shear strength value. Based on this fact, one would expect failure along a {111} surface due to this small incidence angle between the loading direction and {111} plane. Fig. 10 shows the morphology of a typical failure surface obtained on a 45% KOH etched sample. As with the 30% KOH etched sample, failure occurs along the {111} planes forming triangular shapes but on a bank shaped base.

3.2.2. Strength of microridges made with EDP and TMAH solutions

Sample made with EDP and TMAH have the same crystal orientation and overall geometry as did the sample in the previous section. Samples made by EDP produce an average strength value of 9.46 MPa while samples made with TMAH produce 11.1 MPa (see Fig. 7 or Table I). Representative shear strength versus normalized displacement curves for these samples are presented in Fig. 11. Results are similar to those trends reported in Fig. 7 for KOH with the exception that values of TMAH are slightly larger (also with more variation)

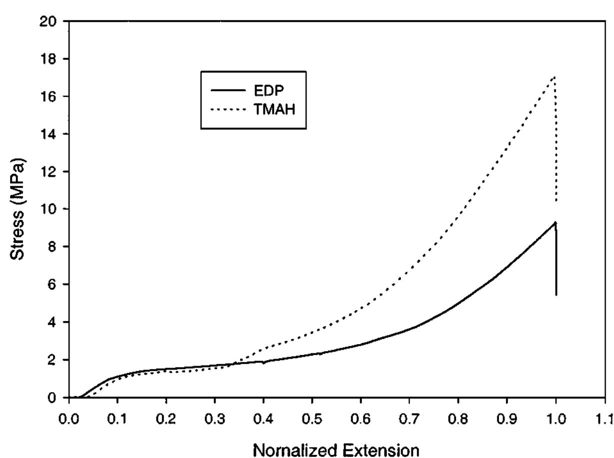

Figure 11 Strength versus normalized displacement of EDP and TMAH.

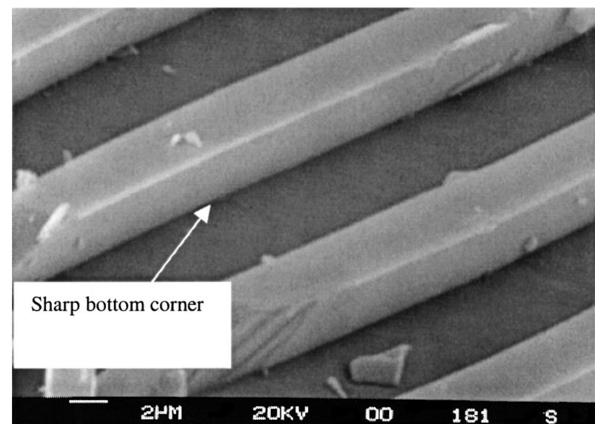

Figure 12 Morphology of broken microridges made by EDP.

than those obtained from the 30% KOH with a similar bottom/sidewall corner geometry. The differences in strengths between EDP and TMAH fabricated microridges as well as the statistical strength variation obtained on TMAH samples can be explained by the morphologies obtained from the fractured surfaces shown in Figs 12 and 13. EDP produces a flat bottom with a relatively reproducible sharp corner (Fig. 12) that appears similar to the geometry produced by 30% KOH (Fig. 2). Therefore, one would expect consistent results between EDP solutions and 30% KOH solution. On the other hand, TMAH produces a bottom (Fig. 13) covered by an irregular "ridge" pattern on {110} plane slightly rougher and perpendicular to the sidewall as explained by Tabata *et al.* [11]. One may argue from this irregular "ridge" pattern that the strength values should vary more significantly for TMAH samples than the KOH or EDP, as indicated by this experimental data.

3.2.3. Strength of microridges made with chlorine RIE and effects of crystal orientations

Dry etching using chlorine RIE produced ridges with substantially higher strengths than those with wet etching processes (Fig. 7 and Table I). In one comparison the crystal orientation was identical to the wet etching approaches (30% KOH, EDP or TMAH) discussed in the preceding section. Furthermore the bottom/sidewall angle (i.e. 90°) is the same (i.e., {110} bottom surface and {111} sidewall made from (110) wafer). While the geometry and crystal orientation were identical, the samples made by chlorine RIE etching produce 95% higher strength values (18.8 MPa) than those by 30% KOH (or EDP and TMAH, previous described). In fact, it's 16% higher than those associated with the "V" shaped bottom fabricated by 45% KOH. We attribute the higher strength to the textured bottom with relative roundness corner produced by RIE etching (Fig. 15a, lower right hand corner).

Chlorine RIE was also used to fabricate microridges with different crystal orientations. We found that crystal orientation of microridges influence strength obviously (Fig. 7 and Table I). Microridges containing a {111} sidewall manufactured from a (110) wafer and

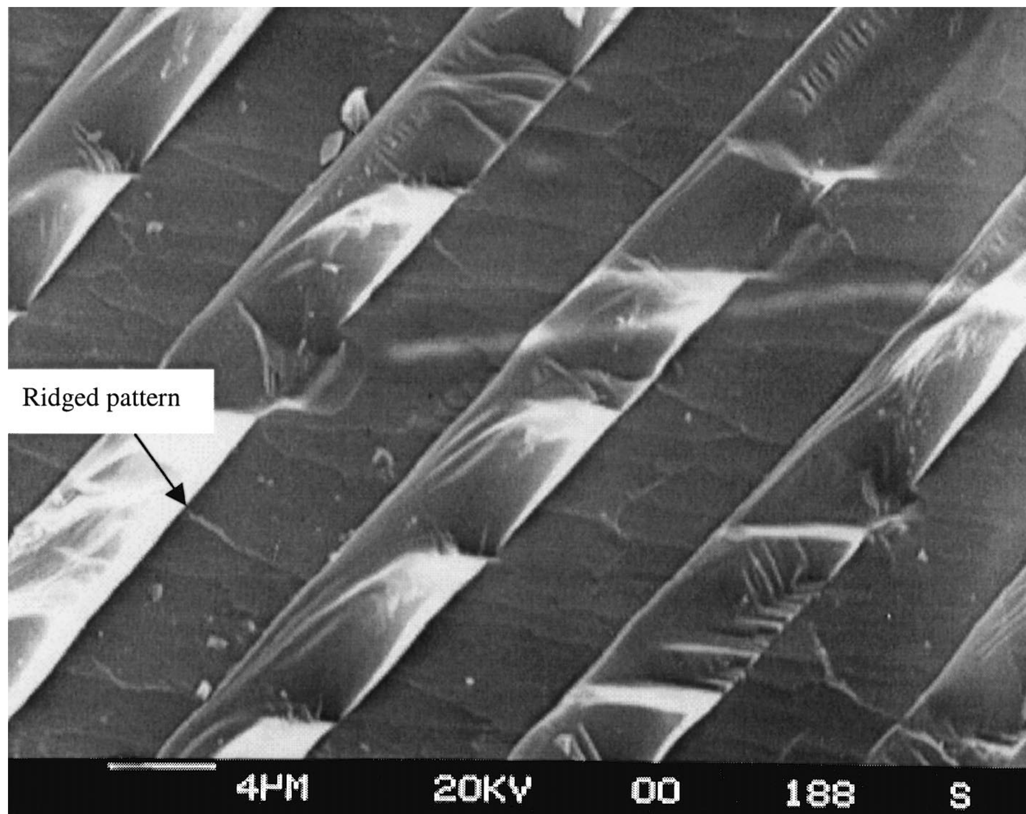

Figure 13 Morphology of broken microridges made by TMAH.

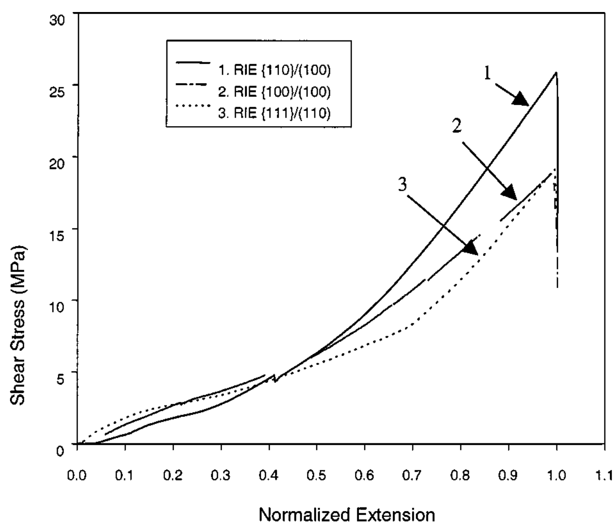

Figure 14 Strength versus normalized displacement of microridges made by chlorine RIE, {110}/(100) means ridges are made on (100) wafer and aligned to {110} plane, etc.

either a {100} sidewall or {110} sidewalls manufactured from a (100) wafer were tested. Test results show that a {110} sidewall plane provides the highest strength (26.4 MPa), followed by the {111} sidewall (18.8 MPa, 29% lower), and finally the {100} sidewall was the lowest (14.6 MPa, 45% lower). The strengths versus normalized displacement curves (Fig. 14) display similar trends to those reported for the wet etching methods KOH (Fig. 8 and Fig. 11). These results clearly indicate that crystal orientation play a prominent role on determining strength.

A SEM micrograph of failure surfaces from a (110) wafer and a (100) wafer are shown in Fig. 15. For {111} sidewall (from (110) wafer), the fracture morphology is similar to the wet etching methods. That is, triangular shapes formed by the {111} planes represent the failure surface (Fig. 15a, upper left hand corner). For the (100) wafer with a {110} sidewall, tilted {111} planes (Fig. 15b, bottom left hand corner) formed the fracture surface. The {111} plane is inclined at an angle of 54.7° with the loading vector and the shear component on {111} plane is 58% of the applied load, a substantial reduction from the (110) wafer with sidewall of {111}. Since the {111} plane is regarded as the sliding plane (or weak plane) of silicon, the (100) wafer with ⟨110⟩ direction loading provides the highest shear strengths for the cases studied here.

For the (100) wafer with a {100} sidewall the {100} sweeping plane intersecting with the tilted {111} edge plane defines the fracture surface. This can be observed in Fig. 15c in the upper right hand corner. This ridge orientation produces the lowest shear strength among the specimens tested for chlorine RIE dry etching. This is due to the lowest tensile strength in ⟨100⟩ direction [7] and large fracture surface of {100} plane is visible in Fig. 15c.

3.2.4. *Strength of microridges made with deep RIE*

We discussed in preceding section that ridges aligned with the {110} plane produced greater strength than the other planes ({111} or {100}) studied in this paper. Based on this result, we fabricated ridges aligned with the {110} plane (largest strength) using deep RIE

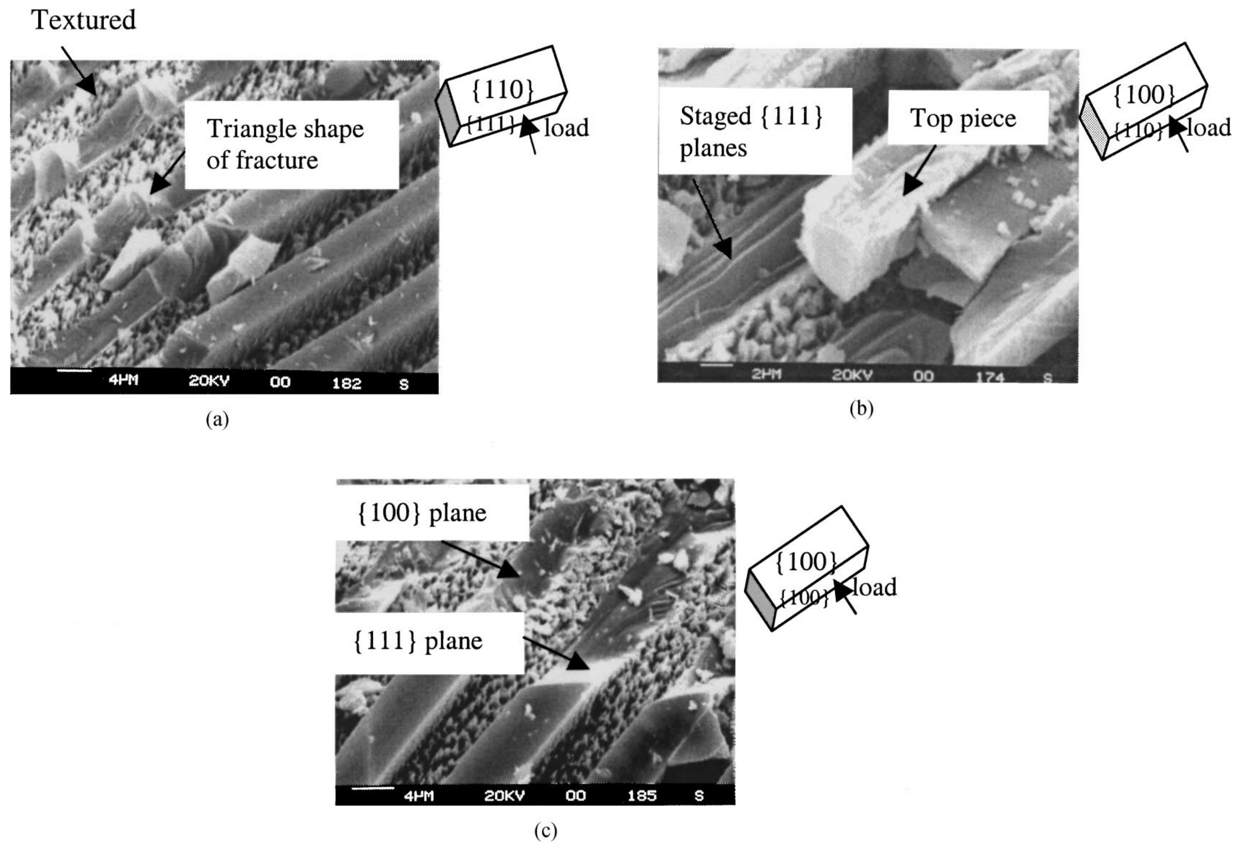

Figure 15 Morphology of broken microridges made with chlorine RIE: (a) (110) wafer with side wall of {111} and loading direction of ⟨111⟩, broken surface intersected by flat {111}; (b) (100) wafer with side wall of {110} and loading direction of ⟨110⟩, broken surface formed by tilted {111}; (c) (100) wafer with side wall of {100} and loading direction of ⟨100⟩, broken surface intersected by edged {111} and large {100} plane.

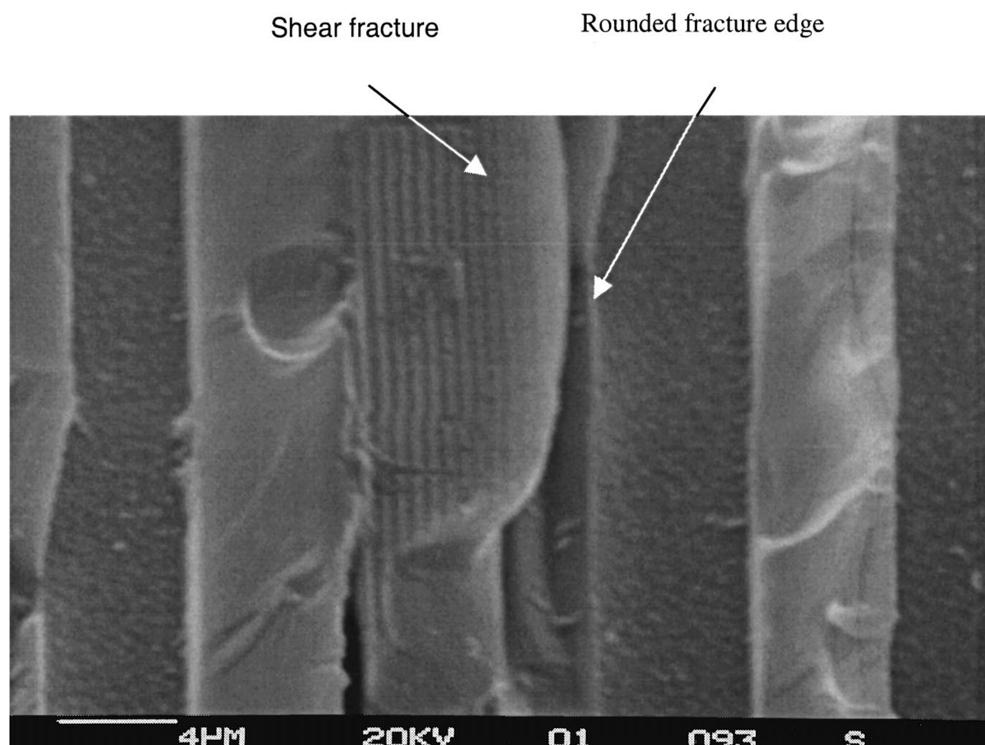

Figure 16 Morphology of broken microridges made by deep RIE.

method. Results for deep RIE indicate that the strength data is 29% higher than chlorine RIE method (34.1 MPa for deep RIE and 26.4 MPa for chlorine RIE, Table I). We attribute this increased strength to the rounded bottom corner produced during this fabrication process (wider bottom angle, Fig. 16, implying lower stress concentration [12]). A rounded fracture boundary is visible in Fig. 16. The fracture ridge in the figure is from the top piece of the engaging pair and shows a pure shear fracture surface with the staged {111} planes.

3.2.5. Strength of trapezoid shape microridges

In this section we will focus on two issues influencing strength values, they are crystal orientation and geometry of microridges, The trapezoid shape has crystal orientation similar to that discussed for deep RIE, i.e., aligning ridges with the intersection of {100}/{110} on a (100) wafer. We begin the discussion by comparing the crystal orientation based on similar fabrication process (30% KOH) described in Section 2.1. Trapezoid ridges were fabricated by using a (100) wafer and aligning with {110} plane. While rectangular ridges were fabricated using a (110) wafer and aligning with {111} plane. The tested strength value of trapezoid ridges is 37.4 MPa (Table I), a value 4 times greater than rectangular microridges made on a (110) wafer (9.6 MPa) with 30% KOH. This difference is attributed to both crystal orientation effects, and local stress concentration (discussed later).

Next we will discuss the results based on similar crystal orientation. They are a composition of 30% KOH (trapezoid ridges) versus chlorine RIE and deep RIE (rectangular ridges). Trapezoid ridges produce 34% higher strength than those fabricated with chlorine RIE (Table I and Fig. 7), and it's similar to those fabricated with deep RIE method (Table I). We attributed these differences in strength to the difference in geometry that will result in different stress concentration level. Simulation results verified also the large difference in strength between trapezoid ridges and rectangular ridges (chlorine RIE) and less difference between trapezoid and rounded rectangular ridges (deep RIE) being attributed to the local stress concentration [14].

4. Summary and conclusion

A summary of the influence of microfabrication processes and crystal orientation on effective shear strength of microridges is shown in Fig. 17. It appears as though fabrication processes produce geometry differences and these geometric features generate substantial variations in strength. For example, ridges with rounded or slopped ("V") shape bottoms produce higher strength then typical rectangular geometry.

In addition to geometry difference crystal orientation played an important role. For example, the microridges of {110} sidewall (made on (100) wafer) has the higher strength than those of {100} and {111} sidewall due to the loading direction (vertical to sidewall) inclining at the largest angle to the {111} plane -sliding plane of silicon. Microridges made with a {100} sidewall produce the lowest strength values among the three. The highest strength was produced with a rounded bottom structure fabricated by deep RIE with a {110} sidewall on a (100) wafer. Trapezoid shape microridges with inclined {111} sidewall on a (100) wafer also produce a similarly large strength value (Fig. 17).

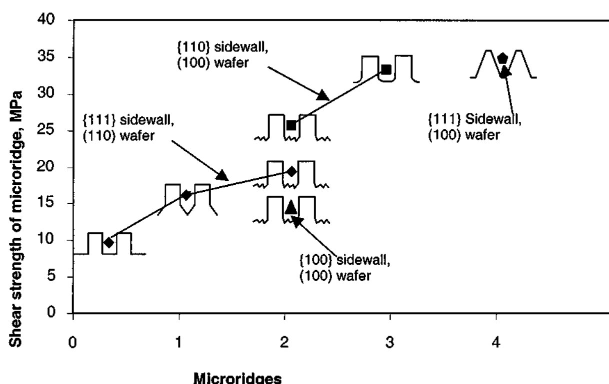

Figure 17 Summary of fabrication and crystal orientation effect on shear strength of microridges.

The effective shear strength of microridges fabricated by commonly used anisotropic wet etching (KOH, TMAH and EDP) and dry etching (chlorine RIE and deep RIE) was measured. The strength values obtained from KOH etchants are concentration dependent. A 45% KOH fabricated structure produced strength values 65% higher than 30% KOH fabricated one. This was attributed to the fact that the former has a tilted bottom ("V" shape, wide-angle corners) resulting in smaller stress concentrations in this critical region. EDP fabricated structures produce strength values similar to the 30% KOH structures, while structure made by TMAH has slightly higher strength values and significantly more variability.

Chlorine RIE produces 95% higher strength values of microridges compared to wet etching with similar geometry of microridges ((110) wafer with {111} sidewall).

Future work will focus on fatigue tests and environmental effects on structural properties.

Acknowledgements

The authors would like to thank Longsun Huang for his contribution to SEM pictures. The authors would also like to acknowledge support by the Army Research Office on a Multidisciplinary University Research Initiative (Contract Number: DAAH04-95-1-0095, Contract Monitor: John Prater).

References

1. Q. CHEN, D. J. YAO, C.-J. KIM and G. P. CARMAN, in Proceedings of the IEEE 11th Annual International Workshop on Micro Electro Mechanical Systems, Heidelberg, Germany, January 1998, p. 384.
2. H. SEIDEL, L. CSEPREGI, A. HEUBERGER and H. BAUMGARTEL, J. of *Electrochemistry Society* **137**(11) (1990) 3612.
3. S. JOHANSSON, J.-A. SCHWEITZ, L. TENERZ and J. TIREN, *J. of Applied Physics* **63**(10) (1988) 4799.
4. T.P. WEIHS, S. HONG, J.C. BRAHMAN and W. D. NIX, *J. of Materials Research* **3**(5) (1988) 931.
5. J. A. CONNALLY and S. B. BROWN, *Science* **256** (12) (1992) 1537.
6. E. H. YANG and H. FUJITA, in Proceedings of International Conference on Solid-state Sensors and Actuators, Transducers'97, Chicago, IL, June 1997, p. 603.
7. K. SATO, M. SHIKIDA, T. YOSHIOKA, T. ANDO and T. KAWABATA, in Proceedings of International Conference on Solid-state Sensors and Actuators, Transducers'97, Chicago, IL, June 1997, p. 595.
8. W. N. SHARPE, JR., B. YUAN, R. VAIDYANATHAN and R. L. EDWARDS, in Proceedings of IEEE 10th Annual International Workshop on Micro Electro Mechanical Systems Workshop, Nagoya, Japan, January 1997, p. 529.

9. K. SATO, M. SHIKIDA and Y. MATSUSHIMA, in Proceedings of IEEE 10th Annual International Workshop on Micro Electro Mechanical Systems Workshop, Nagoya, Japan, January 1997, p. 406.
10. K. SATO, M. SHIKIDA, T. YAMASHIRO, K. ASAUMI, Y. IRIYE and M. YAMAMOTO, in Proceedings of IEEE 11th Annual International Workshop on Micro Electro Mechanical Systems Workshop, Heidelberg, Germany, January 1998, p. 556.
11. O. TABATA, R. ASAHI, H. FUNABASHI, K. SHIMAOKA and S. SUGIYAMA, *Sensors and Actuators A* **34** (1992) 51.
12. F. POURAHMADI, D. GEE and K. PETERSEN, in Proceedings of International Conference on Solid-state Sensors and Actuators, Transducers'91, San Francisco, CA, June 1991, p. 197.
13. J. C. GREEWOOD, *J. Phys. E, Sci. Instrum.* **21** (1998) 1114.
14. L.-H. CHU, Q. CHEN and G. CARMAN, in Proceedings of 1st International Conference on Modeling, Simulation of Microsystems, MSM-99, Puerto Rico, April 1999, p. 489.

Received 27 April 1999
and accepted 4 April 2000